690 镍基合金焊接结晶裂纹形成机理分析

薄春雨，　杨玉亭，　丑树国，　周世锋
（机械科学研究总院 哈尔滨焊接研究所，哈尔滨　150080）

薄春雨

摘　要：采用横向可调拘束试验方法研究了 690 镍基合金焊带堆焊金属的结晶裂纹形成机理。结果表明，690 镍基合金焊接结晶裂纹的形成与晶界（及亚晶界）偏析密切相关，Nb 元素在其中有着重要影响：富 Ni，Nb 低熔点共晶相在晶界（及亚晶界）的偏析，导致堆焊金属的实际结晶温度降低，晶界（及亚晶界）处塑性储备减小、形貌被改善，促使结晶过程中裂纹萌生并沿平直晶界（及亚晶界）扩展。另外，Mn 元素可通过抑制 Nb 元素在晶界的偏析，削弱 Nb 的上述不利作用，增强 690 镍基合金抵抗结晶裂纹的能力。

关键词：690 镍基合金；结晶裂纹；形成机理
中图分类号：TG115.28　　文献标识码：A　　文章编号：0253－360X(2007)10－069－04

0　序　　言

690 镍基合金（0Cr30Ni60Fe10）具有优异的耐应力腐蚀性能。近年来，该材料已在国外开始应用于压水堆核电站蒸汽发生器管板耐蚀层堆焊[1]。690 合金的焊接性相对较差，其中最突出的问题是热裂纹敏感性较大。目前，国外对 690 合金焊接材料的研究已经取得了一定的成果，但就管板耐蚀层堆焊而言，焊接过程中的结晶裂纹问题仍是值得关注的技术关键；同时，对该材料结晶裂纹的形成机理亦没有统一的认识，这对于该材料安全可靠的使用是极为不利的。

试验采用国际上通用的可调拘束试验方法[2－4]，对不同成分配比的 690 合金焊带堆焊金属进行了结晶裂纹敏感性研究；结合显微组织金相试验和扫描电镜断口试验等分析方法，探讨了 690 合金结晶裂纹的形成机理。

1　试　　验

母材试板采用 Q235A 钢板，试板尺寸为 330 mm×140 mm×10 mm。试验焊带经真空冶炼、轧制，规格为 30 mm×0.5 mm，化学成分如表 1 所示。

试验在哈尔滨焊接研究所自行设计的 HHRL－1 型可调拘束试验机上进行，试验过程如图 1 所示。试验前，采用电渣堆焊工艺对母材试板的梯形坡口进行堆焊，经机械矫形平整，加工至试验要求形状尺寸。试验过程中，采用 TIG 电弧沿堆焊金属纵向中心线自 *A* 点～*C* 点进行焊接，焊接至 *B* 点时，对试板施加快速弯曲应变诱发裂纹。通过读数显微镜测量不同应变条件下产生的最大裂纹长度；重复上述焊接过程，采集并记录焊缝金属的结晶温度曲线。

表 1　试验焊带化学成分（质量分数，%）
Table 1　Chemical composition of welding strip

材料编号	Fe	Cr	Ni	Mn	Nb	C	Si	S	P	Al	Ti	余量
1	9.0～11.0	28.5～31.5	基体	1.0～2.0	≤0.5	≤0.030	≤0.20	≤0.010	≤0.010	≤1.0	≤1.0	＜0.5
2	9.0～11.0	28.5～31.5	基体	1.0～2.0	1.0～2.0	≤0.030	≤0.20	≤0.010	≤0.010	≤1.0	≤1.0	＜0.5
3	9.0～11.0	28.5～31.5	基体	1.0～2.0	2.0～3.0	≤0.030	≤0.20	≤0.010	≤0.010	≤1.0	≤1.0	＜0.5
4	9.0～11.0	28.5～31.5	基体	3.0～5.0	≤0.5	≤0.030	≤0.20	≤0.010	≤0.010	≤1.0	≤1.0	＜0.5
5	9.0～11.0	28.5～31.5	基体	3.0～5.0	1.0～2.0	≤0.030	≤0.20	≤0.010	≤0.010	≤1.0	≤1.0	＜0.5
6	9.0～11.0	28.5～31.5	基体	3.0～5.0	2.0～3.0	≤0.030	≤0.20	≤0.010	≤0.010	≤1.0	≤1.0	＜0.5

收稿日期：2007－05－24

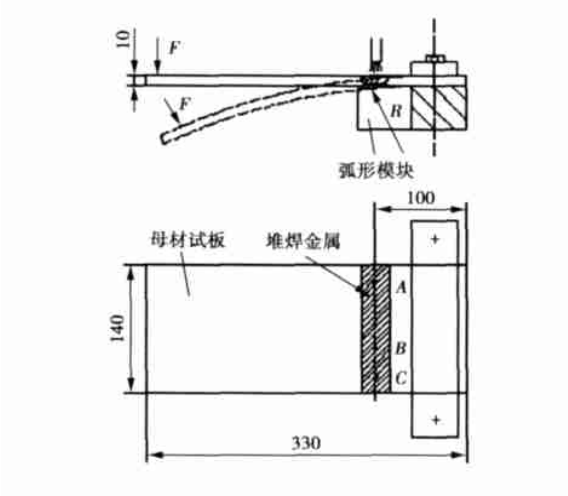

图 1 横向可调拘束试验示意图(mm)

Fig. 1 Trans-Varestraint test

通过可调拘束试验方法,可得到多个裂纹参数,但从不同的角度评定试验材料的裂纹敏感性,大都有一定的局限性。临界应变速率(critical strain rate for temperature drop,简称 CST)是表征结晶过程中焊缝塑性储备情况的物理量[5],而塑性储备是与材料抵抗裂纹的能力一一对应的,故研究选择 CST 作为结晶裂纹敏感性的评定判据。

2 试验结果及分析

2.1 试验结果

通过可调拘束试验得到各试验材料的 CST 值,如图 2 所示。结果表明,对 690 合金堆焊金属而言,随 Nb 含量的增加,CST 值减小,裂纹敏感性增大,尤其是当 Nb 含量大于 2.0%时,抗裂性显著下降;随 Mn 含量的增加,CST 值增大,裂纹敏感性减小。

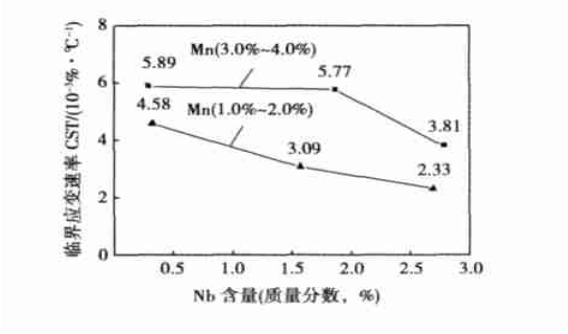

图 2 试验材料的临界应变速率值比较

Fig. 2 CST of 690 alloy welding metal

690 合金焊缝组织中,Nb 元素结合 Ni 元素形成低熔点共晶相的倾向较大,这将导致结晶裂纹敏感性增大。然而,由于 Nb 元素在 690 合金中起着稳定焊缝、增强焊缝金属耐晶间腐蚀性能的重要作用,故该材料含有一定量的 Nb 元素是必须的。密道瓦尔指出[6],在镍基合金焊缝中加入一定含量的 Mn 元素,能够较大程度地抑制 Nb 元素对抗裂性的不利作用。

在各试样断口表面不同区域随机选取 3 组偏析相(每组 3 点,在同一区域),另随机选取基体的 3 个不同位置,采用电子能谱分析每组偏析相的平均 Nb 含量,试验结果如图 3 所示。结果表明,当 690 合金堆焊金属的 Nb 含量处于低(1 号,4 号),中(2 号,5 号)水平时,Mn 元素的加入将一定程度地对 Nb 元素的偏析产生抑制作用,其中,1 号与 4 号两种材料 Nb 元素的平均偏析量分别为 7.51%与 2.66%,2 号与 5 号两种材料 Nb 元素的平均偏析量分别为 18.32%与 8.78%。这与密道瓦尔的观点是一致的。但当 690 合金堆焊金属的 Nb 元素含量达高水平时,Mn 元素的这种作用已不明显,3 号和 6 号两种材料 Nb 元素的平均偏析量分别为 18.72%和 17.71%,差别很小。对比图 2 与图 3 可知,随着 Nb,Mn 含量的变化,试验材料的 CST 与其中 Nb 元素的平均偏析量有着相近的变化趋势,由此可见,690 合金堆焊金属的塑性储备、抗裂性与 Nb 元素的偏析有着直接的联系。

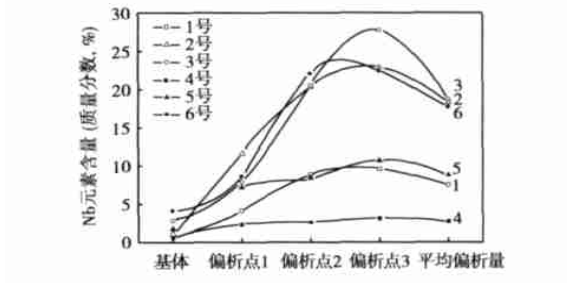

图 3 Mn 元素对裂纹断面 Nb 元素偏析的影响

Fig. 3 Effect of Mn on segregation of Nb in fracture

2.2 690 合金焊带堆焊金属的结晶特性

图 4 所示为试验堆焊金属的显微组织及裂纹断口照片。由图 4a 可以看出,690 合金堆焊金属显微组织中,奥氏体柱状晶粒表面较光滑,晶界平直。堆焊金属结晶过程存在一定的温度梯度,使组织具有很强的方向性,这可以从裂纹断口宏观形貌中得到反映(图 4b),奥氏体柱状晶发达且方向性明显,其方向与热散失的方向是一致的。裂纹断口表现出明显的塑性断裂特征,这可从断口表面的韧窝组织得到反映(图 4c)。

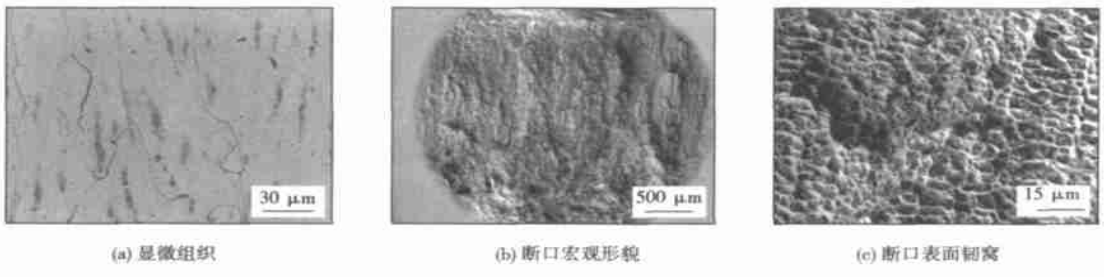

图 4　690 合金焊带堆焊金属结晶特性

Fig 4　Solidification characteristics of 690 alloy welding metal

2.3　690 合金结晶裂纹的分布与形态

横向可调拘束试验条件下，裂纹宏观上围绕固—液相界面分布，一般是焊道中心存在最大裂纹长度。这是由于焊缝结晶的方向性很强，沿热流方向的柱状晶生长的更快更多。因此，同热流方向基本一致的晶界在焊缝中占大多数，绝大部分结晶裂纹与固—液相界面基本垂直。随着裂纹向焊缝中心靠拢，脆性温度区间对应的长度增加，可能出现的裂纹长度相应增大，在焊道中心处产生最大裂纹。如裂纹扩展至焊缝表面，则无金属光泽（图 5a），这是由于裂纹暴露在空气中，高温条件下在表面形成氧化物所致。金相分析表明，大部分裂纹沿晶开裂。多数裂纹的形态是一端较粗钝而另一端较尖锐，如图 5b 所示。另外，在金相试验中发现曲折晶界的存在。图 5c 很好地说明了晶界曲折的作用：晶界曲折打破了裂纹的连续性，故细化晶粒或打乱柱状晶的方向性对改善奥氏体焊缝的抗裂性能有较好的效果。

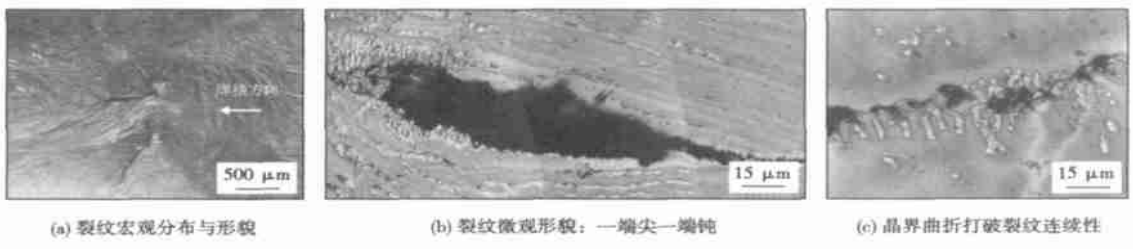

图 5　690 合金焊接结晶裂纹的分布与形貌

Fig 5　Distribution and appearances of solidification cracking in 690 welding metal

2.4　结晶裂纹的形成特性

研究发现，690 合金焊接结晶裂纹的形成与结晶过程中的偏析现象有着密切的联系。焊缝金属结晶速度较快，结晶过程中易于形成晶界或晶内偏析。690 合金中，Ni 含量较高，致使富 Ni 共晶相的形成趋势增大。研究表明，共晶相在晶界（及亚晶界）处的偏析较为严重。图 6a 所示为断口表面晶界颗粒状析出物，从图中可见，颗粒状析出物弥散分布于柱状晶界，较为密集。电子能谱分析结果表明，这些析出物是富 Ni，Nb 的。有研究表明，Ni-Nb 共晶相的熔点较低，平衡条件下仅为 1 175 ℃[7]，在非平衡的焊接条件下则更低。可以确定，这些颗粒状析出物是低熔点共晶相在固态下的存在形式。结晶过程中，由于偏析所造成的焊缝组织不均匀性，表现为晶界上覆盖的低熔点共晶薄膜。图 6b 所示为裂纹断口表面局部区域覆盖的白色薄膜。电子能谱分析结果表明，薄膜的 Nb，Ni 含量较焊缝基体高。可以认为，该薄膜为裂纹产生后仍残留在晶界表面的残余相，是低熔点共晶相在液态下的存在形式。就诱发裂纹而言，薄膜的量是充足的，薄膜厚度较厚。

低熔点共晶相形成元素含量相对较低时，焊缝金属中的偏析程度相应较小。图 6c 所示为 Mn，Nb 含量处于低水平的 690 合金焊缝裂纹断口低温段形貌。从图中可见，断面较为平坦，基体上弥散分布着少量的点状析出物；电子能谱分析表明，该析出物的 Nb 含量仅为 2.09 %，此时 Ni-Nb 共晶相的形成倾向较低，焊缝金属的实际熔点相对较高。

随着共晶相形成元素含量的增加，富 Ni 低熔点共晶相的数量将增加。图 6d 所示为 Nb 含量处于高水平的 690 合金焊缝裂纹断口低温段形貌。从图中

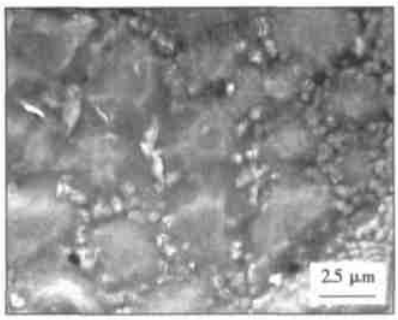

(a) 6号材料晶界析出物

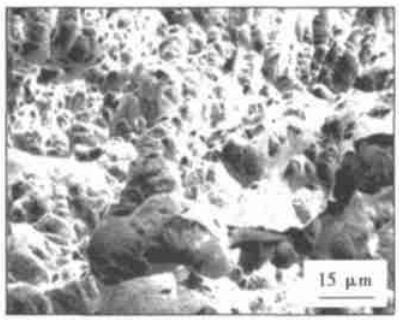

(b) 5号材料断口表面白色薄膜

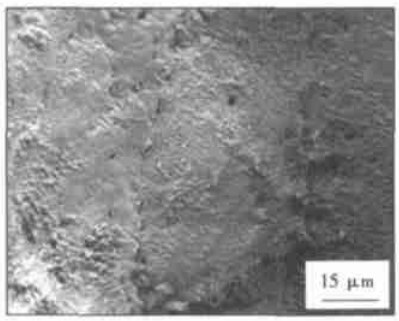

(c) 1号材料断口表面点状析出物

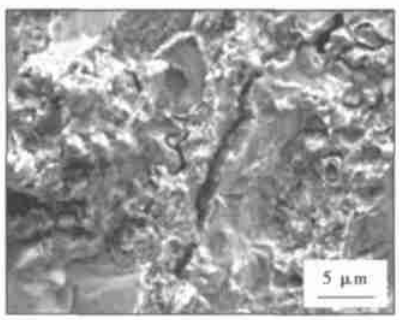

(d) 6号材料断口共晶花样

图 6 典型试样裂纹断口局部形貌

Fig 6 Fracture appearance of typical test specimens

可见，由于 Ni，Nb 等元素含量较高，使断口表面在冷却至低温段后仍残留有较多的共晶花样，这正是共晶液膜处断裂后在低温时的形貌；电子能谱分析表明，共晶花样的 Nb 含量水平达 27.67 %，Ni-Nb 共晶相的量较多。

综上所述，690 合金焊缝结晶裂纹的形成与结晶过程中的偏析现象有着直接联系：低熔点共晶相在结晶过程中偏析于晶界（及亚晶界），使焊缝金属的成分过冷度增大，实际结晶温度区间变宽，促使柱状晶粒长大，晶界（及亚晶界）光滑平直；当焊缝金属中大部分已结晶完成后，晶界（及亚晶界）处的残留低熔点液相趋向于以液态薄膜的形态铺展，成为焊缝金属中的薄弱地带；在焊缝结晶过程中产生的拉应力作用下，薄膜铺展处产生开裂，而此时的液相含量之少使之已无法填塞愈合裂纹，从而裂纹将萌生并沿平直晶界扩展。

3 结 论

（1）690 合金中，Nb 对于抗裂性是不利的。Mn 的加入则可通过抑制 Nb 在晶界的偏析，削弱 Nb 的这种不利作用，增强 690 合金堆焊金属抵抗结晶裂纹的能力。

（2）690 合金结晶裂纹宏观上垂直固—液相界面分布，表面无金属光泽；微观上沿晶分布，大多数裂纹呈一端尖锐一端粗钝的形态。

（3）690 合金结晶裂纹的形成与焊缝结晶过程中的偏析现象有着密切的联系。焊缝金属结晶过程中，富 Ni-Nb 低熔点共晶相在结晶过程中偏析于晶界（及亚晶界），当焊缝金属中大部分已结晶完成后，晶界（及亚晶界）处的低熔点共晶相趋向于以液态薄膜的形态铺展，在焊缝结晶过程中产生的拉应力作用下，薄膜铺展处产生裂纹，而此时的液相含量之少已不足以填塞愈合裂纹，由此裂纹将萌生并沿平直晶界扩展。

参考文献：

[1] 张茂龙. 压水堆核容器中的镍基合金焊接[J]. 锅炉技术，1995(8)：15—20，28.

[2] Savage W F，Lundin C D. The varestraint test[J]. Welding Journal，1965，44(10)：433s—442s.

[3] Nishibata T，Hirata H，Ogawa K，*et al*. Effect of Ni content on weld hot cracking susceptibility of fully austenitic Fe—Cr—Ni alloy[J]. Welding International，2001，15(10)：789—797.

[4] Savage W F，Nippes E F，Goodwin G M. Effect of minor element on hot cracking tendencies of Inconel 600[J]. Welding Journal，1977，56(8)：245s—253s.

[5] 董祖珏，潘永明，王源泉，等. 焊接结晶裂纹敏感性评定指标的研究[J]. 焊接学报，1986，7(9)：139—149.

[6] 密道瓦尔ВИ. 铬镍奥氏体钢的焊接[M]. 成 山，译. 北京：中国工业出版社，1965.

[7] Kuo T Y，Lee H T，Tu C C. Evaluation of effects of niobium and manganese addition on nickel base weldments[J]. Science Technology of Welding and Joining，2003，8(1)：39—48.

作者简介：薄春雨，男，1981 年出生，硕士，助理工程师。主要从事镍基和不锈钢焊接材料的研究与开发。发表论文 2 篇。

Email：bcyhit@163.com

high-temperature tensile test; endurant tensile test

Welding process of micro-alloying cast iron electrode ZHAI Qiuya, ZHAI Bo, TANG Zhen, XU Jinfeng (School of Materials Science and Engineering, Xi' an University of Technology, Xi' an 710048, China). p53—56

Abstract: Using a micro-alloying cast iron electrode the relationship between preheat temperature and microstructure and properties of joint were investigated by backing welding with low-current and then continuous welding with high-current. The results showed that the micro-alloying cast iron electrode has strong graphitizing ability and the weld metal had a little chilling tendency. The applied welding process can effectively decrease the depth of fusion zone and suppress the precipitation of cementite in fusion zone at a great extent. Thus the welding with the micro-alloying cast iron electrode can be realize at ambient temperature. When the preheated temperature is less than 200 ℃, the homogeneous weld can be obtained which has the same microstructure and properties as base metal. With the increase of the preheat temperature, the graphite morphology in weld changes from spotted graphite to rosette graphite to flake graphite. The contents of graphite and ferrite increase while the hardness of the weld decreases. If the preheated temperature reaches to 200 ℃, the microstructure of the weld consists of pearlite, ferrite, flaky graphite and rosette graphite, and the microstructure of fusion zone consists of pearlite, small shiver ferrite and undercooled graphite. The welded joint has excellent mechanical properties.

Key words: micro-alloying cast iron electrode; iron casting; ambient temperature welding; microstructure and properties of joint

Analysis of characteristic of vertical position laser welding for aluminum alloys MIAO Yugang, CHEN Yanbin, LI Liqun, WU Lin (State Key Laboratory of Advanced Welding Production Technology, Harbin Institute of Technology, Harbin 150001, China). p57—60

Abstract: The experiments of vertical and flat position laser welding for 4 mm-thick 5A06 aluminum alloys were implemented, and the characteristics of weld dimension and porosity in the vertical position laser welding for aluminum alloys were investigated. The results show that the concave value and excessive penetration value of vertical welding is less than those of flat welding. Further, with the increase of heat input, the difference of vertical and flat welding becomes obvious. The weld appearance and dimension of the vertical welding and flat welding were slightly different. When the heat input is increased to a great extent, the weld depth of vertical welding is more than that of flat welding. However, the weld width of vertical welding is less than that of flat welding. The porosity of vertical position laser welding for aluminum alloys is composed of the large and irregular porosity or hole. It is not obviously different during vertical welding and flat welding, and a great deal porosity concentrates in the upper and middle part of weld section, which can be indicatied from the distributing position and shape of porosity. The number of porosity in vertical welding was slightly less than that of flat welding for the same welding parametors.

Key words: aluminum alloys; vertical position laser welding; flat welding; characteristic

Effect of aluminizing and diffusion treatment on adhesive strength of arc-sprayed coatings WANG Qiang, LAN Dongyun, XUAN Zhaozhi, LIU Chenghui (College of Materials Science and Engineering, Jilin University, Changchun 130025, China). p61—64

Abstract: Corrosion-resisting and heat-resisting coatings of 18-8 stainless steel were made by arc spraying, aluminizing and diffusion treatment on cast iron. The microstructures and chemical compositions of coatings with aluminizing and diffusion treatment were studied by optical microscope, scanning electron microscope and X-ray diffraction. And the adhesive strength of coatings was evaluated by thermal fatigue tests. The results show that there is some regions with metallurgy bonding on the interface between coatings and substrates through aluminizing and diffusion treatment, therefore, the adhesive strength of coatings were improved greatly. And a long period of aluminizing time is adverse to the adhesive strength of coatings, so aluminizing time should be controlled well.

Key words: arc spraying; aluminizing; diffusion; adhesive strength

Microstructure and melting property of Sn-2.5Ag-0.7Cu-XGe solder MENG Gongge[1], YANG Tuoyu[2], CHEN Leida[1] (1. School of Material Science & Engineering, Harbin University of Science and Technology, Harbin 150040, China; 2. Anhui Science and Technology University, Bengbu, 233100, Anhui, China). p65—68

Abstract: The 3 composition Sn-2.5Ag-0.7Cu-XGe lead-free solders were studied by scanning electron microscope and differential scanning calorimetry equipments. The result indicates that the microstructure is cobblestone-like pro-eutectic grain and scattered long narrow piece and small pellet eutectic mixture. With 0.5% or 1.0% element Ge, the microstructure morphology does not change. But the intermetallic compounds of Ag_3Sn and Cu_6Sn_5 tend to be fine, and their dispersion tends to be well-distributed, and Ag_3Sn phase tends to be fine needle from long narrow piece. By adding element Ge, the temperatures of the melting beginning, the melting peak and the melting finish all reduce correspondingly. And in the melting curve, the endothermic peak changes is narrow, and the melting finish part is long, but the melting temperature zone varies a little.

Key words: lead-free solder; microstructure; melting property

Solidification cracking mechanism of 690 nickeil-based alloy surfacing metal BO Chunyu, YANG Yuting, CHOU Shuguo, ZHOU Shifeng (Harbin Welding Institute, China Academy of Machinery Science and Technology, Harbin 150080, China). p69—72

Abstract: Trans-varestraint test was used to investigate the solidification cracking mechanism of 690 nickel-based alloy surfacing metal. Results show that, the solidification cracking susceptibility of 690 nickel-based alloy surfacing metal is closely correlated with the segregation process during welding, which is greatly influenced by Nb. The solidification temperature of 690 nickel-based alloy surfacing metal falls when the Ni, Nb-rich phases segregate on the grain boundary or subgrain boundary, which induces that the ductility decreases and the appearance is fined. Then, cracking initiates and

expands along the finer grain boundary or subgrain boundary during the solidification process. Furthermore, in 690 nickel-based alloy surfacing metal, Mn weakens the negative influence of Nb on solidification cracking resistance to some extent by restraining the segregation effect of Nb, and then the cracking resistance is improved.

Key words: 690 nickel-based alloy; solidification cracking; mechanism

Characterization on strength and toughness of welded joint for ultra-low carbon bainitic steel GUO Aimin[1,2], LIU Jibin[2], MIAO Kai[2], DONG Hanxiong[2], ZOU Dehui[2], HE Xinlai[1] (1. School of Materials Science and Engineering, Beijing University of Science and Technology, Beijing 100083, China; 2. Research and Development Institute, Wuhan Iron and Steel (Group) Company, Wuhan 430080, China). p73—76

Abstract: The weldability was investigated on ultra low-carbon bainitic steel with thermomechanical control process by utilizing shielded metal arc welding, submerged arc welding and welding thermal simulation test. Results showed that hardness is a little different in the heat affected zone (HAZ). The maximum hardness in the heat affected zone was less than 60 HV. Compared with the same class of low alloy high strength steels, the uniformity of strength in HAZ increases remarkably. The heat affected zone has high toughness. The impact absorbing energy at —40 ℃ reaches above 60 J in the simulated coarse-grained zone when the heat input was 56 kJ/cm. The impact absorbing energy at —40 ℃ reached above 100 J in shielded metal arc welding, and submerged arc welding.

Key words: ultra-low carbon bainitic steel; welding; heat affected zone; toughness

Brazing process of high temperature brazing filler metal BCo45NiCrWB LIU Enze[1,2], SUN Shuchen[1], TU Ganfeng[1], ZHENG Zhi[2], Tong Jian[2], Guo Yi[2] (1. School of Materials and Metallurgy, Northeastern University, Shenyang 110004, China; 2. Superalloys Division, Institute of Metal Research Chinese Academy of Sciences, Shenyang 110016, China). p77—80

Abstract: Wettability and flow-ability experiments of a high temperature brazing filler metal BCo45NiCrWB were studied. Dynamic analysis of brazing process was studied by a STMD-300 surface tension test apparatus. Microstructures of brazed joint with different brazing processes were studied. Microstructure of brazed joint was analyzed by optical microscope. The element distribution of brazed joint was analyzed by electron microprobe. Rupture life of brazed joint at the condition of 980 ℃/132 MPa was tested. The best brazing process of BCo45NiCrWB alloy was established. The brazing parametens are 1 220 ℃/2 h, + 1 080 ℃/4 h+ 900 ℃/16 h, all by argon quench. Results show that the high temperature brazing alloy BCo45NiCrWB has excellent process brazeability. At the condition of 980 ℃/132 MPa the rupture life is more than 60 hours.

Key words: brazing; wettability; flow-ability; rupture life

Effect of thermal cycles of DSAW on microstructure in low alloy high strength steel ZHANG Huajun, ZHANG Guangjun, WANG Junheng, WU Lin (State Key Labortory of Advanced Welding Production Technology, Harbin Institute of Technology, Harbin 150001, China). p81—84

Abstract: According to the low alloy high-strength steel thick plate welding, a new high efficiency technique which does not need back chipping—double-sided double arc welding (DSAW) was provided. Backing run with double-sided double pulsed gas metal arc welding and other passes with double-sided double gas metal arc welding. The temperature fields of single TIG (tungsten inert-gas) welding and DSAW near the bond area were measured by the method of hiding thermal-couple in drilled hole. Compared the thermal cycles of two methods, the $t_{8/5}$ and $t_{8/3}$ of DSAW are higher. In DSAW, fore pass provides the rear pass with a preheat action and rear pass provides the fore pass with a postheat treatment. In single TIG welding, microstructure of weld and coarse grain zone is coarse martensitic, but in DSAW weld contains a few of acicular ferrilite besides of martensitic. Moreover, microstructure of coarse grain zone is smaller than that of single TIG welding. Microhardness distribution results indicated that hardness of DSAW was lower than that of single TIG welding.

Key words: double-sided double arc welding; temperature field; T joint; low alloy high strength steel

Effects of heat treatment on microstructure and properties of electron beam welded TC4 titanium alloy GU Baolan, DING Dawei, WANG Li, XU Xuedong (Institute of Microstructure and Properties of Advanced Material, Beijing University of Technology, Beijing 100022, China). p85—88

Abstract: For electron beam welding (EBW) of TC4 titanium alloy with different preheat treatments and post-weld heat treatment, microstructure and phase composition characteristics of these welds of TC4 were studied by means of optical microscope and X-ray diffraction. Tension and impact test were carried out at room temperature. The results indicated that the microstructure of two kinds of base metals is the mixture of α phasse and β phase, but their state and distribution are different. The post-weld solution and aged operation carried out in the case of annealed welds leads to a coarsening and homogenous of the acicular α, the microstructures is typically reticular structure. The welds in solid solution state were given a relief annealed after welding, whose microstructure at FZ is tempered martensite α in side prior β grains and at grain boundary α. It induced that the ultimate tensile strength (UTS) of annealed state welds is less than that of solution treated welds, but the impact toughness of the former is greater than that of the latter. However, the UTS and impact toughness of these two kinds of welds are greater that that of base metal.

Key words: TC4 titanium alloy; electron beam welding; microstructure; mechanical properties

Finite element analysis simulations of life prediction for PBGA soldered joints under thermal cycling TONG Chuan, ZENG Shengkui, CHEN Yunxia (Reliability Research Institute, Beihang University, Beijing 100083, China). p89—92

Abstract: A typical plastic ball grid array (PBGA) component was selected and the plastic ball grid array packaging was modeled as a tri-layer structure composed of encapsulation, die and substrate. Visco-plastic model was used to describe the behavior of SnPb